Conference paper
Lam, D. and Testo, N. (2008) *Structural design of concrete filled steel elliptical hollow sections.* In: Composite Construction VI, July 2008, July 20-24, 2008, Devil's Thumb Ranch, Colorado, USA.

Composite Construction VI, July 2008, Colorado, USA.

STRUCTURAL DESIGN OF CONCRETE FILLED STEEL ELLIPTICAL HOLLOW SECTIONS

Dr Dennis Lam
School of Civil Engineering
University of Leeds, LS2 9JT, UK
e-mail: d.lam@leeds.ac.uk

Miss Nicola Testo
School of Civil Engineering
University of Leeds, LS2 9JT, UK
e-mail: n.testo@leeds.ac.uk

ABSTRACT

This paper presents the behaviour and design of axially loaded elliptical steel hollow sections filled with normal and high strength concrete. The experimental investigation was conducted with three nominal wall thickness (4mm, 5mm and 6.3mm) and different infill concrete cube strengths varied from 30 to 100 MPa. The effect of steel tube thickness, concrete strength, and confinement were discussed together with column strengths and load-axial shortening curves were evaluated. The study is limited to cross-section capacity and has not been validated at member level. Comparisons of the tests results together with other available results from the literature have been made with current design method used for the design of composite circular steel sections in Eurocode 4 and AISC codes. It was found that existing design guidance for concrete filled circular hollow sections may generally be safely applied to concrete filled elliptical steel tubes.

INTRODUCTION

Concrete filled steel tube (CFST) columns are becoming increasingly popular due to the advantages they offered. They are not only considered aesthetically pleasing but can also offer significant improvement in axial capacity without increases in cross-sectional area being required. Elliptical steel hollow sections represent a recent and rare addition to the range of cross-sections available to structural engineers, however, despite widespread interest in their application, a lack of verified design guidance is inhibiting uptake. The use of elliptical steel hollow section (EHS) with concrete infill is new and innovative, not only provides the advantage mentioned above, but also on the basis of both architectural appeal and structural efficiency. The role of the concrete core is not only to resist compressive forces but also to reduce the potential failure of local buckling by the steel sections. Although local buckling of the steel sections is reduced by the presence of the concrete core, local buckling will still occur to some extent. The concrete core will prevent the steel sections buckling inwards and therefore buckling will generally occur by the outwards buckling of the steel tube. In turn, the steel section reinforced the concrete to resist any tensile forces, bending moments and shear forces and provides confinement to the concrete core. Composite members are of significant interest not only for this reason alone but also for their design suitability in seismic zones [Hajjar, 2000] and their inherent fire resistance [Han et al., 2003]. Existing research on EHS are mainly focused on its behaviour in compression and bending [Gardner and Chan 2007, Chan and Gardner 2007, Zhu and Wilkinson 2006] and also in welded connections [Choo et al 2003, Pietrapertosa and Jaspart 2003, Willibald et al 2006]. Previous research into the structural behaviour and design of concrete filled elliptical hollow sections has been rather limited, with the only reported studies to date by [Zhao et al., 2007]. The results from this study are analysed in this paper.

EXPERIMENTAL STUDY

In order to investigate the behaviour of the elliptical CFSTs, 12 specimens were tested. 150 × 75 mm hot-finished elliptical hollow section (EHS) with 4.0mm, 5.0mm and 6.3mm wall thickness and three nominal concrete strength – C30, C60 and C100 were used for the tests. All specimens were 300mm in length to reduce end effects and to ensure that the specimens behaved as stub columns with little effect from column slenderness. The properties for all the specimens are listed in Table 1.

Table 1: Measured geometric properties of the specimens

Reference	Major axis, outer diameter, 2a (mm)	Minor axis, outer diameter, 2b (mm)	Wall thickness, t (mm)	Steel area, A_s (mm^2)	Concrete area, A_c (mm^2)
150×75×4	150.40	75.60	4.18	1471.5	-
150×75×4-C30	150.40	75.60	4.18	1471.5	7458.6
150×75×4-C60	150.57	75.52	4.19	1475.8	7455.0
150×75×4-C100	150.39	75.67	4.18	1471.8	7466.0
150×75×5	150.23	75.74	5.08	1773.8	-
150×75×5-C30	150.12	75.65	5.12	1785.5	7133.9
150×75×5-C60	150.23	75.74	5.08	1773.8	7162.8
150×75×5-C100	150.28	75.67	5.09	1777.1	7154.2
150×75×6.3	148.78	75.45	6.32	2164.1	-
150×75×6.3-C30	148.78	75.45	6.32	2164.1	6652.3
150×75×6.3-C60	148.92	75.56	6.43	2202.1	6635.5
150×75×6.3-C100	149.53	75.35	6.25	2149.1	6700.0

Testing of the composite columns was carried out using a 3000kN capacity ToniPACT testing machine and the experimental set up is shown in Figure 1. Both ends of the specimens were milled flat and capped with rigid steel plate in order to distribute the applied load uniformly over both the concrete and steel section for the composite loaded columns. The specimens were loaded at 50kN intervals at the beginning of the test (i.e. in the elastic region) and at a loading rate of 10kN intervals after the column began to yield, in order to have sufficient data points to delineate the “knee” of the stress-strain curve. A linear variable differential transducer (LVDT) was used to monitor the vertical deformation. All of the operation and the change of loading rate were operated manually and all the readings were recorded when both load and strain had been stabilized. After the immediate drop of the load due to local buckling, the test continued until excessive deformation of the column was observed. After the test, the specimens were removed, photographed and carefully examined.

Figure 1: Test arrangement and instrumentations

Concrete Properties

Three nominal concrete strengths – C30, C60 and C100 were studied. The concrete was produced using commercially available materials with normal mixing and curing techniques; the three mix designs are shown in Table 2 together with the cube and cylinder strength at test day. The strength development of the concrete was monitored over a duration of 28 days by conducting periodic cube and cylinder tests – the results of the cube tests are illustrated in Figure 2. Additionally, at the time of each series of stub column tests, two further standard cube tests and two standard cylinder tests were performed.

Table 2: Concrete mix proportions (% by weight) and the compressive strength (test day)

Grade	Cement	Fines	Coarse	w/c ratio	Silica fume	Super-plasticiser	f_{cu} (N/mm^2)	f_{ck} (N/mm^2)
C30	1.0	2.5	3.5	0.65	0	0	36.9	30.5
C60	1.0	2.0	3.3	0.40	0	0	59.8	55.3
C100	1.0	1.5	2.5	0.30	0.1	0.03	98.4	102.2

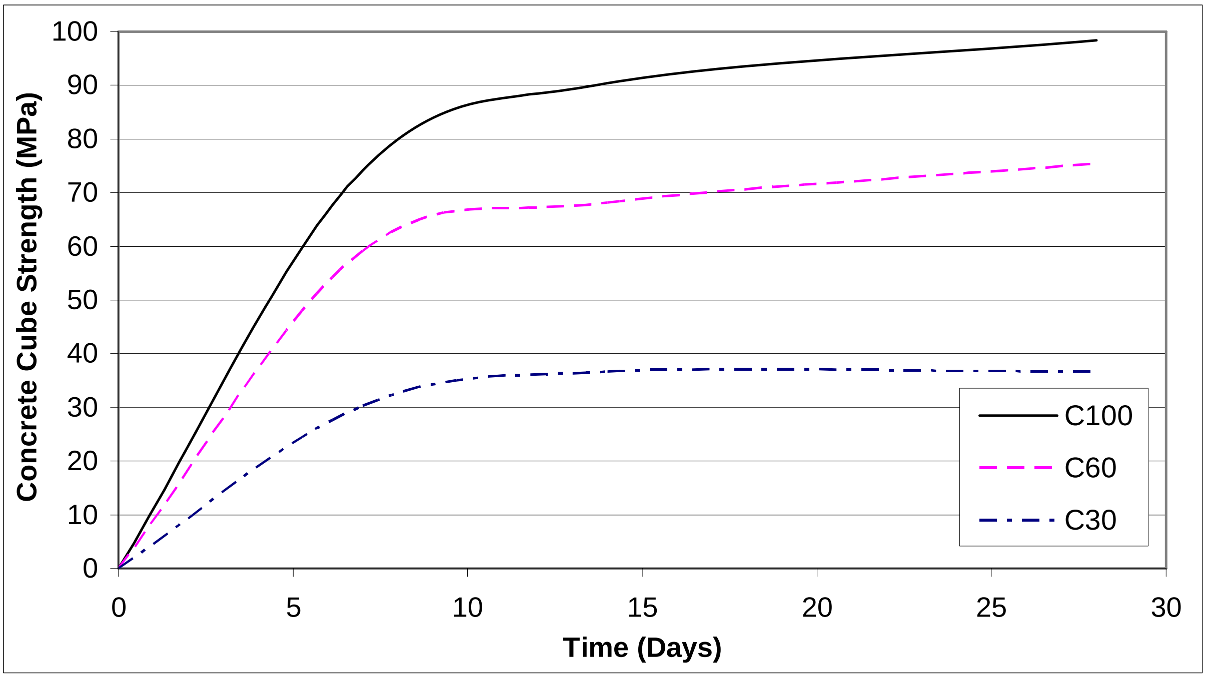

Figure 2: Concrete development strength

Steel Properties

Coupons were cut from the EHS and tested to [EN10002-1 2001] to determine the tensile strength. The coupons were cut form the in the region of maximum radius of curvature (i.e. the flattest portion of the section) and milled to specification. Some flattening of the ends occurred while gripping the specimen but this was well away from the ‘neck’ of the sample. The results from the coupon tests are summarized in Table 3.

Table 3: Steel properties of the EHS

Specimens	Young’s modulus E (N/mm^2)	Yield stress f_y (N/mm^2)	Ultimate strength f_u (N/mm^2)
150×75×4	217500	376.5	513
150×75×5	217100	369.0	505
150×75×6.3	216500	400.5	512

TEST RESULTS

All the specimens were tested under axial compression until failure. The typical failure modes of the composite specimens are shown in Figure 3. For the unfilled EHS, both inward and outward local buckling was observed in the deformed specimen while for the filled tubes, although inward buckling was prevented by the concrete core, outward local buckling is clearly evident in the deformed specimens.

Figure 3: Typical failure mode of the composite EHS

The load vs. end shortening curves from the EHS stub column tests are shown in Figures 4 to 6. The results show the clear advantage of composite EHS columns over their bare (unfilled) EHS counterparts. Overall, it may be observed from Figures 4 to 6 that the stockier EHS tubes with lower concrete strengths have more ductility, though enhancements in load carrying capacity beyond that of the bare steel sections due to concrete filling are more significant for slender sections with higher concrete strengths. The ultimate loads from the stub columns tests $N_{u,Test}$ are presented in Tables 4 with the composite factor, ϕ. The level of strength enhancement (beyond that of the unfilled tubes) can be represented by the composite factor, ϕ, the definition of which is given by Eq. (1). This index provides a quantitative measure of the benefit arising from concrete-filling.

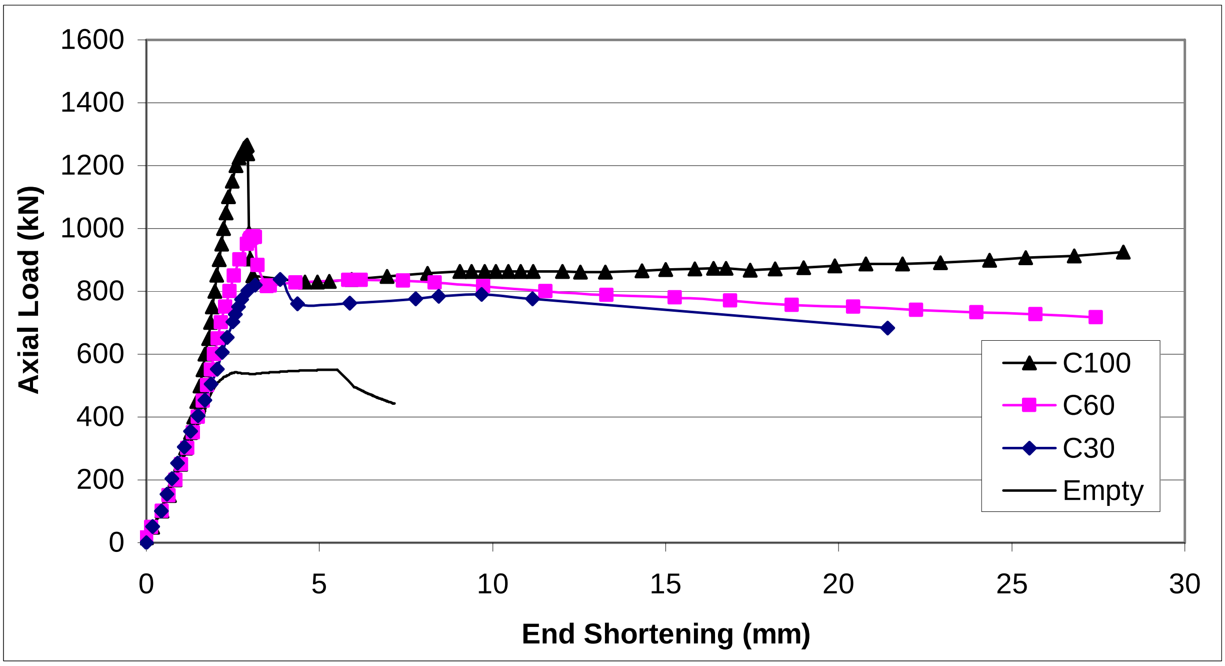

Figure 4: Axial load vs. end shortening curves for 150×75×4 EHS composite columns

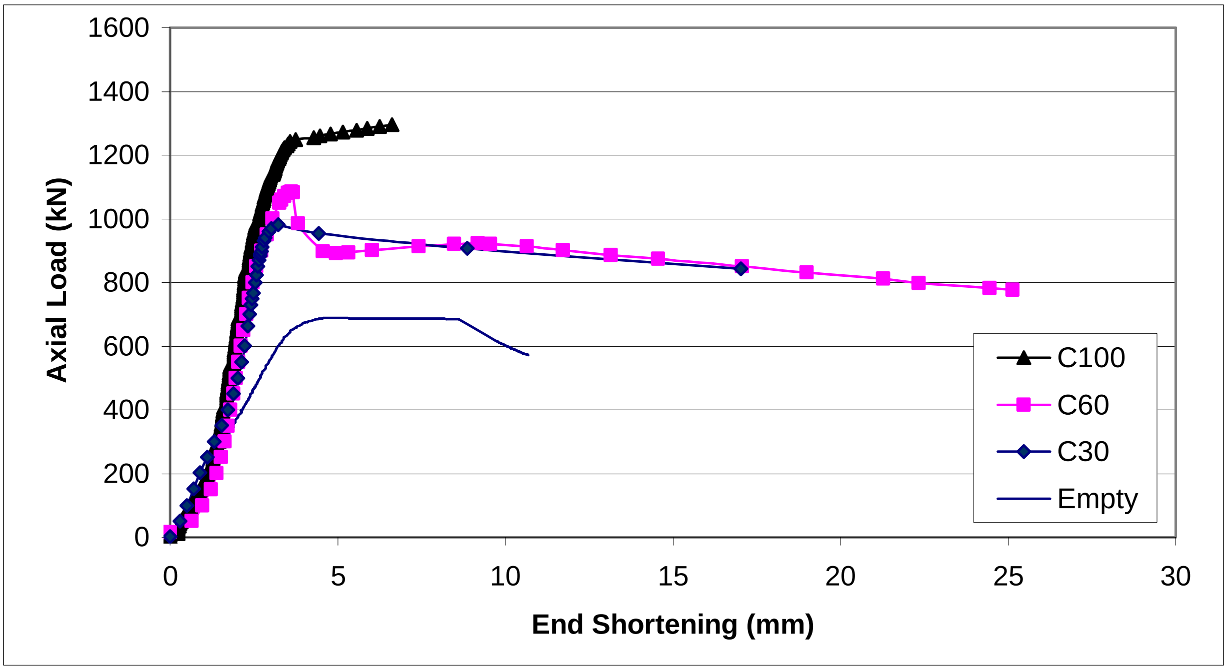

Figure 5: Axial load vs. end shortening curves for 150×75×5 EHS composite columns

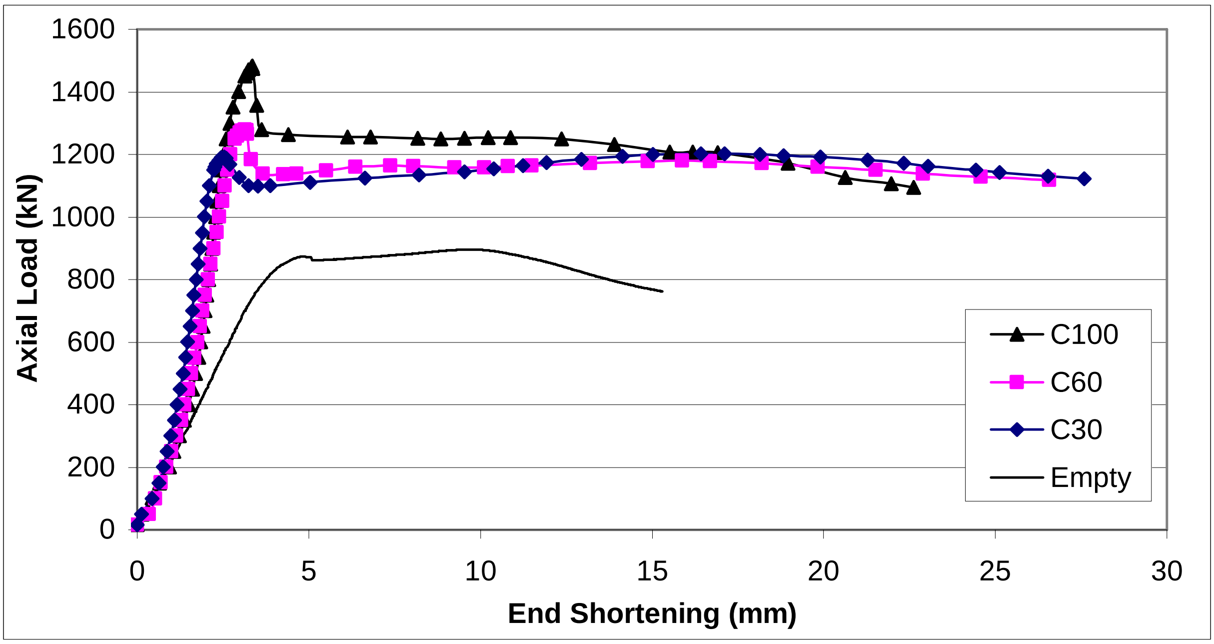

Figure 6: Axial load vs. end shortening curves for 150×75×6.3 EHS composite columns

Table 4: Summary of test results and composite factor, ϕ

Reference	$N_{u,\ Test}$	Composite factor, ϕ
150×75×4	550.0	1.00
150×75×4-C30	838.6	1.52
150×75×4-C60	974.2	1.77
150×75×4-C100	1264.6	2.30
150×75×5	688.9	1.00
150×75×5-C30	981.4	1.42
150×75×5-C60	1084.1	1.57
150×75×5-C100	1296.0	1.88
150×75×6.3	871.8	1.00
150×75×6.3-C30	1202.9	1.38
150×75×6.3-C60	1280.1	1.47
150×75×6.3-C100	1483.2	1.70

$$\phi = \frac{N_{\text{u,filled}}}{N_{\text{u,unilled}}} \qquad (1)$$

Where,

$N_{u,filled}$ is the ultimate resistance of the concrete-filled elliptical test specimens;
$N_{u,\ unfilled}$ is the ultimate test resistance of the corresponding empty EHS.

Figure 7 shows the relationship between the composite factor, ϕ and the cube strength of the concrete f_{cu} for the three different tube thicknesses. The results show that, as expected, the concrete contribution ratio increases for the higher concrete strengths, and that the level of enhancement is more significant for the thinner tubes; the 4mm elliptical tube shows a doubling in capacity with the C100 concrete infill.

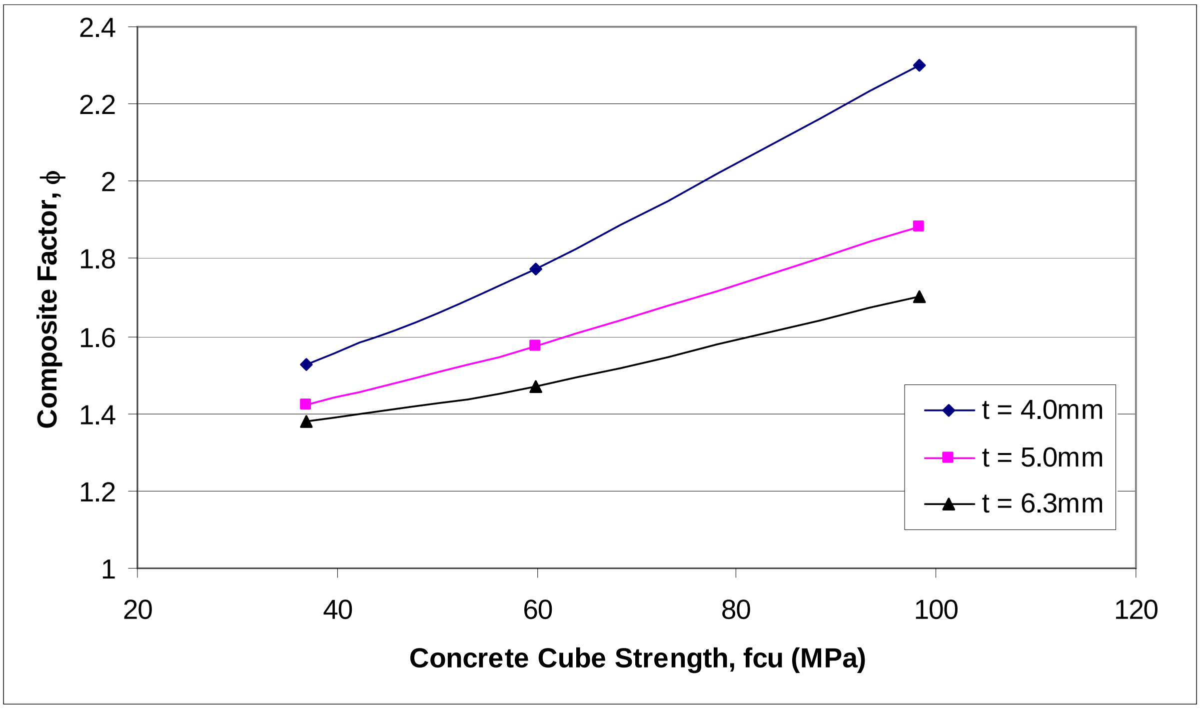

Figure 7: Composite factor vs. concrete cube strength curves

DESIGN CODE

Concrete-filled elliptical hollow sections are not explicitly covered by current design codes. The test results obtained in the present study have been combined with those reported by [Zhao et al., 2007] and compared with existing design guidance for the circular concrete-filled tubes. The codes considered are [EN 1994-1-1 2004] and [AISC 360-05 2005] respectively abbreviated to EC4, and AISC in this paper. The principal differences between the codes relate to the factors that are applied to the individual steel and concrete contributions to the composite resistance. Following the comparisons, design recommendations are made for concrete-filled elliptical hollow sections.

EC4 covers concrete encased and partially encased steel sections and concrete-filled tubes with and without reinforcement. The compressive resistance $N_{u,EC4}$ of concrete-filled steel tubes is given by Eq. (2). This is the latest design code that takes into account increases in concrete capacity due to confinement by the steel sections.

$$N_{u,EC4} = \eta_a A_a f_{yd} + A_c f_{cd}\left(1 + \eta_c \frac{t}{d}\frac{f_y}{f_{ck}}\right) \tag{2}$$

Where,

$N_{u,EC4}$	Ultimate axial capacity of the composite column
f_{cd}	Design compressive strength of the concrete
f_{ck}	Cylinder strength of concrete
f_y	Yield strength of the steel tube
f_{yd}	Design strength of the steel tube
d	Larger diameter of the elliptical steel section
t	Thickness of steel tube
η_c	Coefficient of concrete confinement
η_a	Coefficient of steel confinement

In the AISC code, the compressive resistance of concrete-filled circular hollow sections $N_{u,AISC}$ is given by Eq. (3). The 0.95 factor on the concrete contribution in Eq. (3) reflects the superior performance of concrete-filled CHS over their rectangular counterparts.

$$N_{u,AISC} = A_s f_y + 0.95 A_c f_{ck} \tag{3}$$

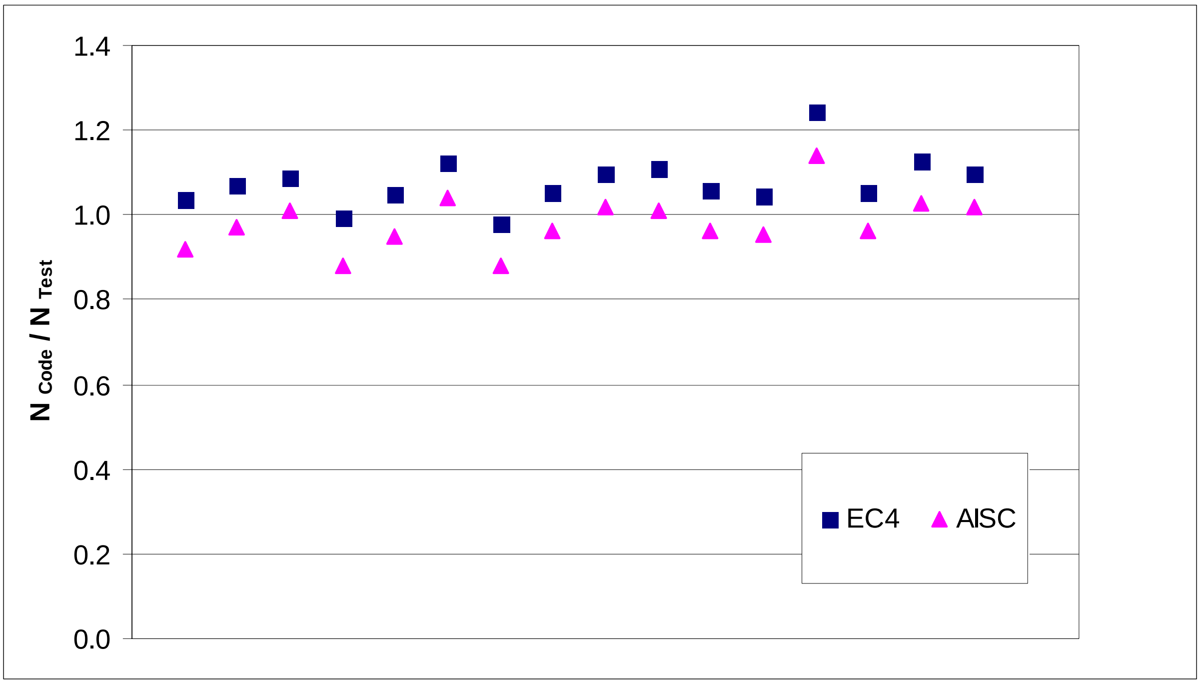

Figure 8: Comparison of code prediction

Table 5: Comparison between test results and codes prediction

Reference	$N_{u, Test}$ (kN)	$N_{u, EC4}$ (kN)	$\frac{N_{u,EC4}}{N_{u,Test}}$	$N_{u,AISC}$ (kN)	$\frac{N_{u,AISC}}{N_{u,Test}}$
150×75×4-C30	838.6	871.7	1.04	770.1	0.92
150×75×4-C60	974.2	1046.6	1.07	947.3	0.97
150×75×4-C100	1264.6	1379.1	1.09	1279.0	1.01
150×75×5-C30	981.4	977.8	1.00	865.6	0.88
150×75×5-C60	1084.1	1140.7	1.05	1030.8	0.95
150×75×5-C100	1296.0	1459.2	1.13	1350.4	1.04
150×75×6.3-C30	1202.9	1184.6	0.98	1059.5	0.88
150×75×6.3-C60	1280.1	1354.2	1.06	1230.5	0.96
150×75×6.3-C100	1483.2	1630.1	1.10	1511.2	1.02
150×75×4-C60*	1075	1193.1	1.11	1087.9	1.01
150×75×5-C60*	1163	1229.5	1.06	1118.4	0.96
150×75×6.3-C60*	1310	1370.3	1.05	1247.8	0.95
200×100×5-C60*	1598	1991.3	1.25	1819.4	1.14
200×100×6.3-C60*	2068	2181.4	1.05	1989.5	0.96
200×100×8-C60*	2133	2404.7	1.13	2193.3	1.03
200×100×10-C60*	2290	2514.9	1.10	2331.2	1.02
		Mean	1.08	Mean	0.98
		SD	0.061	SD	0.064

*Test reported by [Zhao et al., 2007]

All the test results presented in this paper have been combined with those reported by [Zhao et al. 2007] and compared with the predictions from the aforementioned design codes. The comparisons, shown in Figure 8 and Table 5 reveal that the ultimate test loads from the 16 concrete-filled EHS specimens are generally over-predicted by the EC4 formulations for concrete-filled CHS by 8% and underestimated by 2% by the corresponding AISC concrete-filled CHS formulations. On the basis of the comparisons, it is recommended that the AISC expression for concrete-filled CHS (Eq. (3)) is most suitable for predicting the resistance of concrete-filled EHS. However, it is clear that the level of confinement and hence the resistance of concrete-filled EHS are related to the aspect ratio of the section and further research to investigate this feature is ongoing.

CONCLUSIONS

A total of 12 tests – 9 compositely loaded and 3 unfilled EHS have been performed to investigate the compressive behaviour of concrete-filled elliptical hollow sections. The compressive response was found to be sensitive to both steel tube thickness and concrete strength, with higher tube thickness resulting in higher load-carrying capacity and enhanced ductility, and higher concrete strengths improving load-carrying capacity but reducing ductility. The experimental results from the present study were combined with an additional 7 experimental results from literature, and compared with existing code provisions for circular hollow sections. From the comparisons, it may be concluded that existing design rules for concrete-filled CHS may be safely applied to EHS, and that the AISC design expression for CHS provide an accurate prediction of composite EHS behaviour.

ACKNOWLEDGEMENTS

The authors would like to thank Dr Leroy Gardner of Imperial College for his time and help with the research work and Corus for providing the steel specimens used in this research project. The skilled assistance provided by the technical staff in the School of Civil Engineering at Leeds University is also appreciated.

REFERENCES

AISC 360-05 (2005), Specification for structural steel buildings, American Institute of Steel Construction.

Chan, T. M. and Gardner, L (2008), Compressive resistance of hot-rolled elliptical hollow sections, Engineering Structures, 30, pp. 522 – 532.

Choo, Y.S., Liang, J.X. and Lim, L.V. (2003), Static strength of elliptical hollow section X-joint under brace compression, 10th. Int. Symposium on Tubular Structures, Madrid, Spain, pp. 253 – 258.

EN 10002-1 (2001). Metallic materials – Tensile testing – Part 1: Method of test at ambient temperature, British Standard Institute.

EN 1994-1-1 (2004), Eurocode 4: Design of composite steel and concrete structures - Part-1-1: General rules and rules for buildings, British Standard Institute.

Gardner, L. and Chan, T. M. (2007), Cross-section classification of elliptical hollow sections, Journal of Steel and Composite Structures, 7(3), pp. 185 – 200.

Hajjar, J.F. (2000), Concrete filled steel tube columns under earthquake loads, Progress in Structural Engineering and Materials, 3(1), pp. 72 – 81.

Han, L.H., Yang, Y.E. and Xu, L. (2003), An experimental study and calculation on the fire resistance of concrete-filled SHS and RHS columns, Journal of Constructional Steel Research, 59(4), pp. 427 – 452.

Pietrapertosa, C. and Jaspart, J.-P. (2003), Study of the behaviour of welded joints composed of elliptical hollow sections, 10th. Int. Symposium on Tubular Structures, Madrid, Spain, pp. 601 – 608.

Willibald, S., Packer, J.A. and Martinez-Saucedo, G. (2006), Behaviour of gusset plate connections to ends of round and elliptical hollow structural section members, Canadian Journal of Civil Engineering, 33, pp.373 – 383.

Zhao, X. L., Lu, H. and Galteri, S. (2007). Tests of Elliptical Sections Filled with SCC (Self-Compacting Concrete). Proceedings of the 5th International Conference on Advances in Steel Structures. Singapore, pp. 950 – 955.

Zhu, Y. and Wilkinson, T. (2006), Finite element analysis of structural steel elliptical hollow sections in pure compression, 11th. Int. Symposium on Tubular Structures, Québec City, Canada, pp. 179 – 186.